Involvement of NADPH oxidases in the Na/K-ATPase/Src/ROS oxidant amplification loop in renal fibrosis

HUIMIN ZHANG[1-5*], FANGFANG LAI[6*], XI CHENG[2-5,7] and YU WANG[1-5]

[1]Renal Division, Department of Medicine, Peking University First Hospital; [2]Institute of Nephrology,
Peking University; [3]Key Laboratory of Renal Disease, National Health and Family Planning Commission of The P.R. China;
[4]Key Laboratory of Chronic Kidney Disease Prevention and Treatment, Ministry of Education; [5]Research Units of Diagnosis
and Treatment of Immune-Mediated Kidney Diseases, Chinese Academy of Medical Sciences, Beijing 100034;
[6]State Key Laboratory of Bioactive Substances and Functions of Natural Medicines, Institute of Materia Medica, Chinese
Academy of Medical Sciences and Peking Union Medical College, Beijing 100050; [7]Department of Nephrology,
Tianjin Medical University General Hospital, Tianjin 300070, P.R. China

Abstract. The Na/K-ATPase/Src complex is reportedly able to affect reactive oxygen species (ROS) amplification. However, it has remained elusive whether NADPH oxidases (NOXs) are involved in this oxidant amplification loop in renal fibrosis. To test this hypothesis, interactions between oxidative features and Na/K-ATPase/Src activation were examined in a mouse model of unilateral urethral obstruction (UUO)-induced experimental renal fibrosis. Both 1-tert-butyl-3-(4-chlorophenyl)-1H-pyrazo lo[3,4-d]pyrimidin-4-amine (PP2) and apocynin significantly attenuated the development of UUO-induced renal fibrosis. Apocynin administration attenuated the expression of NOXs and oxidative markers (e.g., nuclear factor erythroid 2-related factor 2, heme oxygenase-1,4-hydroxynonenal and 3-nitrotyrosine); it also partially restored Na/K-ATPase expression and inhibited the activation of the Src/ERK cascade. Furthermore, administration of PP2 after UUO induction partially reversed the upregulation of NOX2, NOX4 and oxidative markers, while inhibiting the activation of the Src/ERK cascade. Complementary experiments in LLC-PK1 cells corroborated the *in vivo* observations. Inhibition of NOX2 by RNA interference attenuated ouabain-induced oxidative stress, ERK activation and E-cadherin downregulation. Thus, it is indicated that NOXs are major contributors to ROS production in the Na/K-ATPase/Src/ROS oxidative amplification loop, which is involved in renal fibrosis. The disruption of this vicious feed-forward loop between NOXs/ROS and redox-regulated Na/K-ATPase/Src may have therapeutic applicability for renal fibrosis disorders.

Introduction

Renal fibrosis is the final common pathological feature of most forms of kidney disease, leading to irreversible renal function impairment (1-4). Src kinase belongs to the non-receptor tyrosine kinase family. Activated Src has been implicated in the regulation of numerous intracellular signaling cascades (e.g., MAPK, PI3K and protein kinase C) and cellular processes such as cell proliferation, differentiation, migration and invasion (5-8). Among the numerous kinases that function as signaling hubs, Src has a critical role in renal fibrosis through the integration of multiple fibrogenic signal inputs (9,10). In addition to its well-known ion pump function, Na/K-ATPase has been identified as an important regulator of Src activation through the formation of an Na/K-ATPase/Src complex, particularly in epithelial cells (11,12). pNaKtide, a polypeptide derived and constructed from the ND1 segment of the Na/K-ATPase α1 subunit, is able to mimic Na/K-ATPase and bind to the kinase domain of Src, preventing its activation without affecting the pump function of Na/K-ATPase (13). A previous study by our group indicated that the inhibition of Src and its downstream signaling cascades by pNaKtide attenuated unilateral ureter obstruction (UUO)-induced renal fibrosis, indicating that Na/K-ATPase/Src complex-regulated signaling pathways are involved in renal fibrosis (10).

Ouabain and other cardiotonic steroids are specific Na/K-ATPase ligands. Oxidative stress, represented by reactive oxygen species (ROS) production, has been observed upon activation of the Na/K-ATPase/Src complex by cardiotonic steroids in various cell types (14,15). In addition, there have been reports that ROS can activate Na/K-ATPase/Src signaling cascades with further generation of intracellular ROS (16-18). This leads to a feed-forward oxidative amplification

Correspondence to: Dr Yu Wang, Renal Division, Department of Medicine, Peking University First Hospital, 8 Xishiku Street, Xicheng, Beijing 100034, P.R. China
E-mail: ddwangyu@sina.com

*Contributed equally

loop of Na/K-ATPase/Src/ROS; ROS are generated by Na/K-ATPase/Src complex activation and they enhance Na/K-ATPase/Src signaling cascade activation (12,15). This oxidative amplification loop has been observed in disease models such as uremic cardiomyopathy, cognitive decline and neurodegeneration, salt-sensitive hypertension and obesity (19-23). In the above-mentioned study, increased ROS production was observed in UUO mice, which was attenuated by pNaKtide (10); those findings provided support for the hypothesis that an Na/K-ATPase/Src/ROS oxidant amplification loop is involved in renal fibrosis.

The molecular mechanisms of ROS generation involved in the oxidant amplification loop have not been fully elucidated thus far, to the best of our knowledge. Nicotinamide adenine dinucleotide phosphate oxidases (NOXs) have been regarded as a major source of ROS in the kidney in various animal models (24-27). A previous study by our group observed increased expression levels of both NOX2 and NOX4 soon after UUO induction, accompanied by increased expression levels of oxidative stress markers (28). The administration of apocynin, an inhibitor of NOXs, decreased the expression levels of NOX2, NOX4 and oxidative stress markers, indicating that NOXs are major contributors to oxidative stress in UUO animals (29). The present study investigated whether NOXs serve as a major source of ROS in the Na/K-ATPase/Src/ROS oxidant amplification loop, which is potentially involved in renal fibrosis.

Materials and methods

Reagents and antibodies. Monoclonal antibodies to phosphorylated extracellular signal-related kinase (p-ERK; cat. no. sc-7383), ERK (cat. no. sc-514302), c-Src (cat. no. sc-8056), α-smooth muscle actin (α-SMA; cat. no. sc-32251), p47phox (cat. no. sc-17845), p67phox (cat. no. sc-374510), 8-hydroxy-2'-deoxyguanosine (8-OHdG; cat. no. sc-66036) and NOX2 (cat. no. sc-130548) were obtained from Santa Cruz Biotechnology, Inc.; monoclonal antibodies to collagen I (COL-I; cat. no. ab270993), Na/K-ATPase (cat. no. ab7671) and 3-nitrotyrosine (3-NT; cat. no. ab61392) were obtained from Abcam; monoclonal antibodies to GAPDH (cat. no. 2118S), polyclonal antibodies to p-Src (cat. no. 2101s) and horseradish peroxidase-conjugated anti-rabbit (cat. no. 7074) and anti-mouse antibodies (cat. no. 7076) were acquired from Cell Signaling Technology, Inc.; a monoclonal antibody to 4-hydroxynonenal (4-HNE; cat. no. MA5-27570) was purchased from Thermo Fisher Scientific, Inc.; and monoclonal antibodies to nuclear factor E2-related factor 2 (Nrf2; cat. no. 16396-1-AP), heme-oxygenase 1 (HO-1; cat. no. 66743-1-Ig), NOX1 (cat. no. 17772-1-AP), NOX4 (cat. no. 14347-1-AP) and NOX5 (cat. no. 25350-1-AP) were purchased from Proteintech Group, Inc. An enhanced chemiluminescence kit was purchased from Merck KGaA. Furthermore, 1-tert-butyl-3-(4-chlorophenyl)-1H-pyrazolo[3,4-d]pyrimidin-4-amine (PP2) was purchased from Selleck Chemicals; and ouabain, apocynin and N-acetylcysteine (NAC) were obtained from Sigma-Aldrich (Merck KGaA). RIPA lysis buffer and a ROS Assay Kit (cat. no. S0033M) were obtained from Beyotime Institute of Biotechnology. Medium199 and fetal bovine serum were purchased from Thermo Fisher Scientific, Inc.; a Sirius Red Staining Kit (cat. no. AG1470-2) was purchased from Acmec Biochemical Co., Ltd. Small interfering RNAs (siRNAs) specific for NOX2 were obtained from Hanbio Biotechnology Co., Ltd. with the following sequences: 5'-GUGCACCAUGAUGAGGAGA-3' (sense) and 5'-UCUCCUCAUCAUGGUGCAC-3' (antisense). Scrambled siRNA sequences were as follows: 5'-UUCUCC GAACGUGUCACGU-3' (sense) and 5'-ACGUGACACGUU CGGAGAA-3' (antisense).

Experimental animals and treatment. All animal studies were approved by the Animal Experimentation Ethics Committee of Peking University First Hospital (Beijing, China; no. J2022005) and complied with the Guide for the Care and Use of Laboratory Animals published by the National Institutes of Health. Male C57BL/6J mice (age, 6-8 weeks; weight, 18-23 g) were purchased from the Institute of Laboratory Animal Science, Chinese Academy of Medical Sciences and housed at 25°C with 40% humidity and a 12-h light/dark cycle. They were provided with free access to sterile water and food. The UUO model was established as previously described (10,30). All animals were anesthetized by intraperitoneal injection of 50 mg/kg pentobarbital sodium. The left ureter was exposed and ligated with 4-0 silk sutures. In sham-operated mice, the ureter was mobilized but not ligated. Animals were randomly divided into the following six groups: Sham surgery, sham + PP2, sham + apocynin, UUO, UUO + PP2 and UUO + apocynin. Apocynin (100 mg/kg) was administered by gavage immediately after surgery and then daily for 7 days. PP2 (2 mg/kg) was intraperitoneally administered immediately after ureteral ligation and then daily for 7 days. On day 7 after surgery, the pre-specified experimental endpoint, the mice were sacrificed through complete exsanguination under anesthesia induced by intraperitoneal administration of 50 mg/kg pentobarbital sodium and the left kidneys were harvested. Death was confirmed when the animals' respiration and heartbeat ceased. Every effort was made to minimize animal suffering during the procedure. The harvested kidneys were decapsulated and then rapidly dissected. Coronal sections (2-3 mm thick) through the middle portion of the kidney were fixed in 10% neutral buffered formalin and embedded in paraffin; the remaining kidney tissue was snap-frozen in liquid nitrogen for further analysis.

Histological and immunohistochemical staining of the kidney. Histological staining of collagen fibers was performed on formalin-fixed and paraffin-embedded tissues using the Sirius Red Staining kit in accordance with the manufacturer's protocol. Immunohistochemical staining was conducted as described in previous studies by our group (10,28). In brief, deparaffinized serial sections were rehydrated in PBS and subjected to antigen retrieval by microwave heating (1,400 W, 3 min, 30 sec). After natural cooling, sections were washed with PBS and incubated with 0.3% hydrogen peroxide for 15 min at room temperature to block endogenous peroxidase activity; they were subsequently incubated with 3% bovine serum albumin for 30 min at 37°C in a humidified chamber. Sections were incubated overnight at 4°C with primary antibodies to COL-I (dilution, 1:200), α-SMA (dilution, 1:1,000),

NOX2 (dilution, 1:200), NOX4 (dilution, 1:200), 8-OHdG (dilution, 1:1,000) and Na/K-ATPase (dilution, 1:500). As a negative control, PBS was used instead of a primary antibody. After tissues had been washed with PBS, they were incubated with horseradish peroxidase-conjugated anti-mouse/rabbit IgG polymer (cat. no. PV6000; ZSGB-BIO, Ltd.) for 1 h at room temperature. Results were visualized using diaminobenzidine and sections were observed under a microscope (Leica DM2500; Leica Microsystems GmbH). Images were captured at a magnification of x40 and then analyzed using ImageJ software [Version 1.53t; National Institutes of Health (NIH)].

Cell culture and treatments. The pig renal proximal tubule cell line LLC-PK1 was obtained from the American Type Culture Collection. The cells were cultured in Medium199 containing 3% fetal bovine serum, 100 units/ml penicillin and 100 mg/ml streptomycin at 37°C in a humidified incubator with 5% CO_2. After the cells had reached 80-90% confluence, they were serum-starved overnight and then exposed to further treatments as indicated in the figure legends. Certain cells were pre-treated with PP2 (5 μM) or NAC (3 mM) for 30 min prior to ouabain treatment (100 nM, 30 min).

siRNA transfection. LLC-PK1 cells were cultured to 50-60% confluence and then transfected with siRNA oligonucleotides that specifically targeted NOX2 (80 nM) using Lipofectamine 3000 (Thermo Fisher Scientific, Inc.), in accordance with the manufacturer's instructions. As a control, scrambled siRNA (80 nM) lacking homology to any gene in the vertebrate transcriptome was transfected into LLC-PK1 cells in a separate dish. After transfection, cells were cultured for 48 h and then used for experiments.

Measurement of intracellular ROS. Intracellular ROS levels were detected using a ROS Assay Kit, in accordance with the manufacturer's instructions. LLC-PK1 cells were seeded in black 96-well culture plates ($5x10^3$ cells/well) and incubated with diacetyldichlorofluorescein diacetate (10 μM) for 20 min at 37°C. After cells had been washed with PBS, they were treated with ouabain (100 nM, 30 min) with or without pretreatment with PP2 (5 μM) or NAC (3 mM) for 30 min. Dichlorofluorescein fluorescence intensity was measured by a microplate reader (Bio Tek Synergy H1; Agilent Technologies, Inc.) at an excitation wavelength of 488 nm and an emission wavelength of 525 nm. Simultaneously, fluorescence images were acquired by fluorescence microscopy.

Western blot analysis. Kidney tissue samples and LLC-PK1 cell homogenates were prepared and analyzed as previously described (10,17). In brief, tissue and cell samples were lysed with RIPA lysis buffer containing a mixture of phosphatase and protease inhibitors (Beyotime Institute of Biotechnology). After homogenization, the lysates were centrifuged; supernatants were collected for western blot analysis. Equal amounts of protein extracts were subjected to SDS-PAGE (10%) and transferred onto polyvinylidene difluoride membranes (Millipore; Merck KGaA). After membranes had been blocked with 5% skimmed milk in Tris-buffered saline plus Tween-20 (TBS-T) for 1 h at room temperature, they were incubated overnight at 4°C with the indicated primary antibodies. Antibodies to

E-cadherin, p67phox, NOX1 and HO-1 were used at a dilution of 1:2,500; other primary antibodies were used at a dilution of 1:1,000. Subsequently, the membranes were washed with TBS-T and then incubated with horseradish peroxidase-conjugated secondary antibodies (dilution, 1:2,500) for 1 h at room temperature. Next, western blots were developed with enhanced chemiluminescence reagents and visualized using an Image Quant LAS 4000 mini (Cytiva). ImageJ software (Version 1.53t, NIH) was used for densitometric analysis of western blots. Band intensities were calculated according to area and pixel value. For quantification, the target protein content was normalized against the corresponding GAPDH signal, for each experiment. The ratio was then expressed relative to the content of the sham kidney *in vivo* experiment or the control group, where applicable, which was normalized to 1 in each experimental repeat.

Statistical analysis. Data shown in graphs represent the mean ± SEM for each group. All experiments were performed at least three times. Comparisons between two groups were performed using unpaired Student's t-test. One-way analysis of variance was used for multi-group comparisons, followed by Tukey's post-hoc test. P<0.05 was considered to indicate a statistically significant difference.

Results

PP2 and apocynin treatment attenuate UUO-induced renal fibrosis and myofibroblast accumulation. UUO resulted in renal fibrosis onset, as determined by Sirius Red staining (Fig. 1A), and collagen-I expression, as determined by immunohistochemical staining and homogenates analysis via western blotting (Fig. 1B and D; P<0.001 vs. sham alone). Administration of either PP2 or apocynin significantly prevented fibrosis in UUO mice (Fig. 1A, B and D; both P<0.05 vs. UUO alone). Administration of either PP2 or apocynin to sham surgery mice did not significantly affect the degree of renal fibrosis.

α-SMA is regarded as a myofibroblast marker. In addition to changes in extracellular matrix deposition, UUO induced significant myofibroblast accumulation in the renal interstitium (determined by immunohistochemical staining) and in kidney homogenates (determined by western blot analysis) (Fig. 1C and E; P<0.001 vs. sham alone). Administration of either PP2 or apocynin reduced myofibroblast accumulation in UUO mice (Fig. 1C and E; both P<0.001 vs. UUO alone). No significant effects of PP2 or apocynin treatment were observed in sham surgery mice. These findings indicated that the activation of Src and NOXs contributes to myofibroblast accumulation in renal interstitium and renal fibrosis onset after UUO injury.

Effects of apocynin administration on Na/K-ATPase expression and Src/ERK activation. The level of Na/K-ATPase expression is able to regulate Src activation (17). Therefore, changes in Na/K-ATPase expression in the kidney were investigated. UUO led to a significant decrease in Na/K-ATPase expression at 7 days postoperatively (Fig. 2A and B; P<0.001 vs. sham alone). Significant activation of Src and ERK1/2 was also observed in kidney homogenates from UUO mice
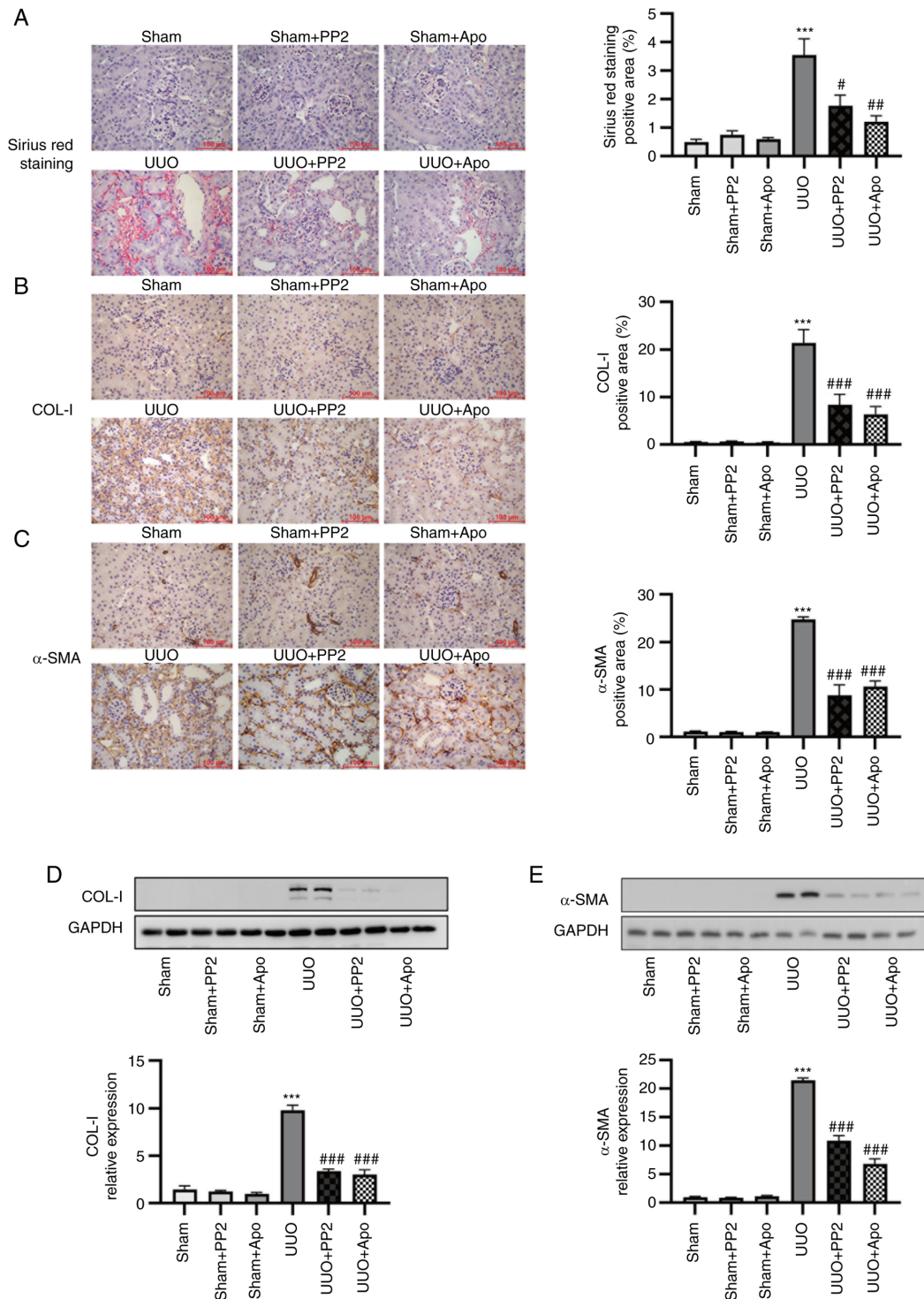
Figure 1. UUO-induced renal fibrosis and myofibroblast accumulation are attenuated by PP2 and apocynin treatment. (A) Representative images and data analysis of Sirius Red renal histology. (B) Representative images and data analysis of immunohistochemical staining for COL-I. (C) Representative images and data analysis of immunohistochemical staining for α-SMA (magnification, x400; scale bars, 100 μm). (D) Representative western blot and data analysis of COL-I expression in kidney homogenates. (E) Representative western blot and data analysis of α-SMA expression in kidney homogenates. Values are expressed as mean ± SEM (n=3-5). ***P<0.001 vs. sham alone; #P<0.05, ##P<0.01, ###P<0.001 vs. UUO alone. COL-I, collagen I; α-SMA, α-smooth muscle actin; PP2, 1-tert-butyl-3-(4-chlorophenyl)-1H-pyrazolo[3,4-d]pyrimidin-4-amine; Apo, apocynin; UUO, unilateral ureteral obstruction.

(Fig. 2C and D; P<0.001 vs. sham alone). In UUO mice, apocynin treatment partially but significantly reversed the decrease in Na/K-ATPase expression and inhibited Src and ERK activation (Fig. 2; both P<0.05 vs. UUO alone). By contrast, PP2 treatment reduced Src and ERK1/2 activation in obstructed kidneys (Fig. 2C and D; both P<0.001 vs. UUO alone) but

did not significantly influence the UUO-induced decrease in Na/K-ATPase expression.

Src inhibition attenuates UUO-induced changes in oxidative stress profiles. Compared with the sham group, UUO significantly increased activation of the Nrf2/HO-1 pathway and
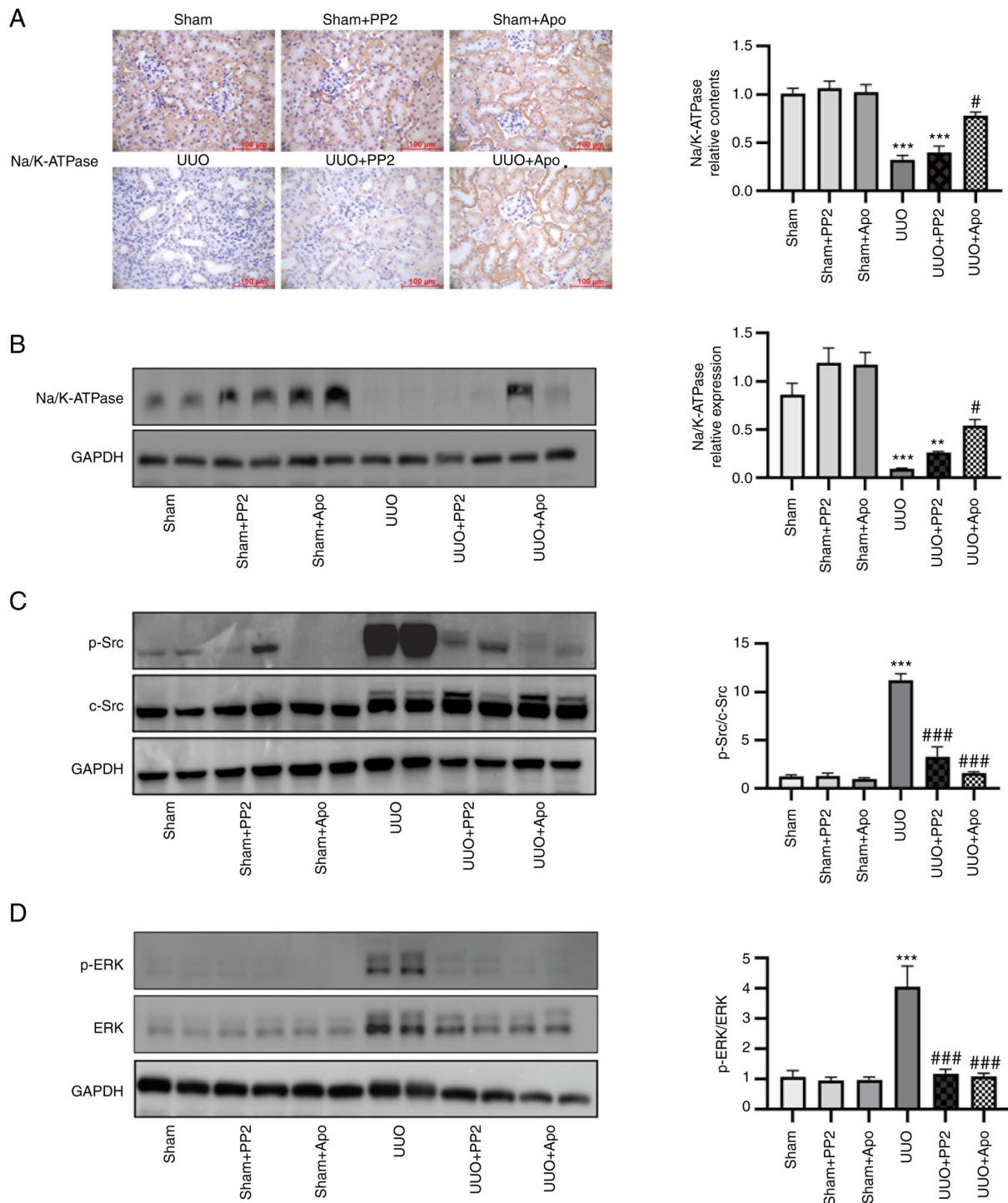
Figure 2. Apocynin treatment downregulates Na/K-ATPase expression and inhibits Src/ERK activation. (A) Representative images and data analysis of immunohistochemical staining for Na/K-ATPase (magnification, x400; scale bars, 100 μm). (B) Representative western blot and data analysis of Na/K-ATPase expression in kidney homogenates. (C) Representative western blot and data analysis of Src activation in kidney homogenates. Src activation was expressed as the p-Src/t-Src ratio. (D) Representative western blot and data analysis of ERK activation in kidney homogenates. ERK activation was expressed as p-ERK/t-ERK. Values are expressed as the mean ± SEM (n=3-5). **P<0.01, ***P<0.001 vs. sham alone; #P<0.05, ###P<0.001 vs. UUO alone. Apo, apocynin; UUO, unilateral ureteral obstruction; p-, phosphorylated; t-, total.

the levels of oxidative stress biomarkers 3-NT and 4-HNE in kidney homogenates, as determined by western blot analysis (Fig. 3A and B; all P<0.01 vs. sham alone). Another oxidative stress biomarker, the DNA oxidation product 8-OHdG, was also increased in the kidneys of UUO mice, as determined by immunohistochemical staining (Fig. 3C; P<0.001 vs. sham alone). Administration of PP2 significantly inhibited

Nrf2/HO-1 axis activation and 3-NT/4-HNE/8-OHdG expression in obstructed kidneys with similar effects to apocynin (Fig. 3; all P<0.05 vs. UUO alone), suggesting that Src activation contributed to the development of oxidative stress in UUO mice. Collectively, these findings support the involvement of an Na/K-ATPase/Src/ROS oxidative amplification loop in UUO-induced renal fibrosis.
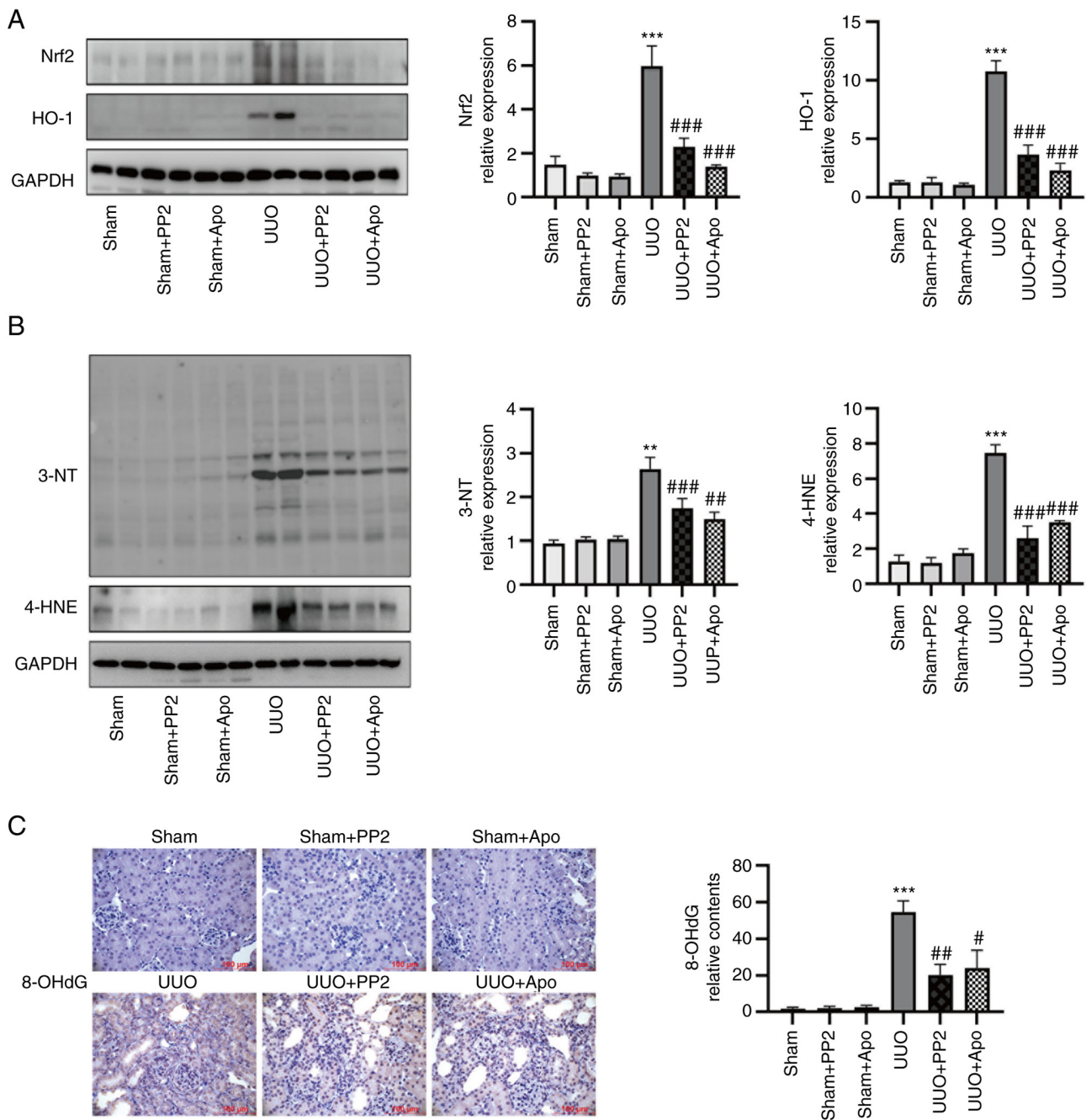
Figure 3. Src inhibition decreases expression levels of Nrf2, HO-1, 3-NT and 4-HNE. (A) Representative western blot and data analysis of Nrf2 and HO-1 content in kidney homogenates. (B) Representative western blot and data analysis of 3-NT and 4-HNE content in kidney homogenates. (C) Representative images and data analysis of immunohistochemical staining of 8-OHdG (magnification, x400; scale bars, 100 μm). Values are expressed as the mean±SEM (n=3-5). **P<0.01, ***P<0.001 vs. sham alone; #P<0.05, ##P<0.001, ###P<0.001 vs. UUO alone. 3-NT, 3-nitrotyrosine; 4-HNE, 4-hydroxynonenal; 8-OHdG, 8-hydroxy-2'-deoxyguanosine; Apo, apocynin; HO-1, heme-oxygenase 1; Nrf2, nuclear factor E2-related factor 2; UUO, unilateral ureteral obstruction.

Involvement of NOXs in oxidative stress generation in UUO-induced renal fibrosis. Considering that NOXs have key roles in the production of ROS in various models (24-27), the expression levels of NOX2 and NOX4 were examined. As presented in Fig. 4, the expression levels of both NOX2 and NOX4 were significantly increased (both P<0.001 vs. sham alone) in UUO mouse kidneys, as determined by immunohistochemical staining and western blot analysis. PP2 treatment significantly attenuated the expression of NOX2 and NOX4 in UUO mice (Fig. 4; both P<0.05 vs. UUO alone), consistent with the changes in oxidative stress markers described above.

In addition, administration of apocynin significantly inhibited the activation of NOX2 and NOX4 (Fig. 4; both P<0.01 vs. UUO alone). These results suggested that NOX activation contributes to the Na/K-ATPase/Src/ROS oxidative amplification loop in UUO mice.

Effects of ouabain on ROS production and Na/K-ATPase/Src signaling pathway in LLC-PK1 cells. Ouabain is a prototypic agonist of Na/K-ATPase. When the Na/K-ATPase/Src complex is activated by ouabain, Src functions as a master upstream regulator of intracellular signaling pathways (17,18).
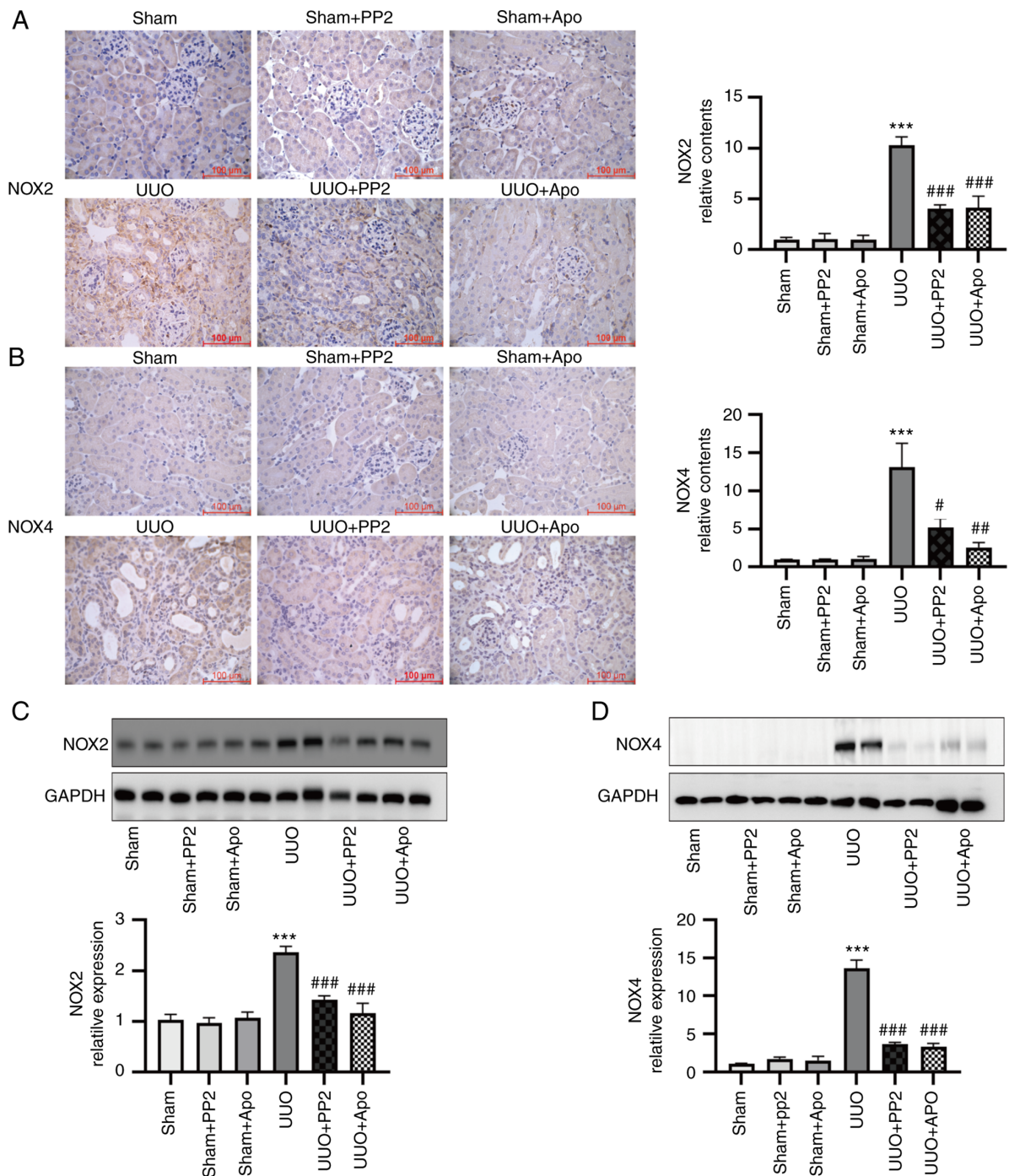
Figure 4. Expression levels of NOX2 and NOX4 are reduced by PP2 and apocynin treatment. (A) Representative images and data analysis of immunohisto-chemical staining of NOX2. (B) Representative images and data analysis of immunohistochemical staining of NOX4 (magnification, x400; scale bars, 100 μm). (C) Representative western blot and data analysis of NOX2 expression in kidney homogenates. (D) Representative western blot and data analysis of NOX4 expression in kidney homogenates. Values are expressed as the mean ± SEM (n=3-5). ***P<0.001 vs. sham alone; #P<0.05, ##P<0.01, ###P<0.001 vs. UUO alone. Apo, apocynin; UUO, unilateral ureteral obstruction; NOX, NADPH oxidase.

As indicated in Fig. 5A and B, ouabain (100 nM) caused significant activation of Src and ERK1/2 in LLC-PK1 cells between 15 min and 1 h post-treatment. A concomitant increase in intracellular ROS levels was observed during ouabain treatment (Fig. 5C and D). Based on these results, 30 min was selected as the observation time-point in subsequent cell experiments.

To investigate the roles of ROS in Src-regulated signaling pathways, ouabain-induced signaling was assessed in the presence and absence of the Src inhibitor PP2 and the antioxidant NAC. Under basal conditions, PP2 and NAC treatments did not influence Src/ERK1/2 activation or ROS production. Pretreatment with PP2 (5 μM, 30 min) attenuated the ouabain-induced activation of Src and ERK, as well as the ouabain-induced production of ROS (Fig. 6A-D). Pretreatment of cells with NAC (3 mM, 30 min) reduced ouabain-induced ROS production and ouabain-induced activation of ERK1/2, but it had no effect on ouabain-induced activation of Src (Fig. 6E-H). These results suggested that
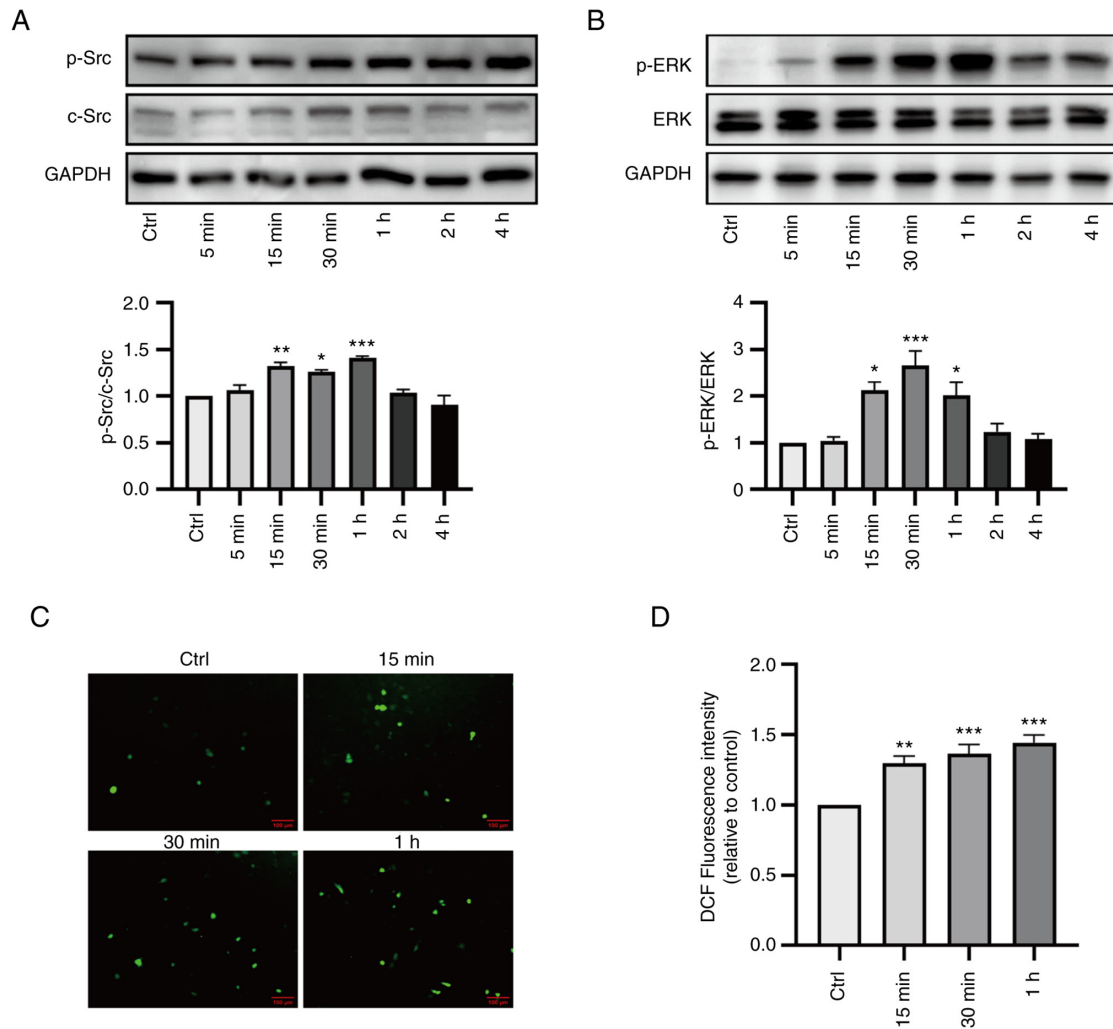
Figure 5. Ouabain-induced ROS production in LLC-PK1 cells. (A) Time course of Src activation. Src activation was expressed as the p-Src/t-Src ratio. (B) Time course of ERK activation. ERK activation was expressed as the p-ERK/t-ERK ratio. (C) Representative fluorescence images of ROS production in ouabain-treated LLC-PK1 cells (scale bars, 100 μm). (D) DCF fluorescence intensity in ouabain-treated LLC-PK1 cells, as determined with a microplate reader. Representative western blots and quantitative data are provided. Values are expressed as the mean ± SEM (n=3). *P<0.05; **P<0.01; ***P<0.001 vs. Ctrl. Ctrl, control; p-, phosphorylated; t-, total; ROS, reactive oxygen species; DCF, dichlorofluorescein.

Na/K-ATPase/Src activation is upstream of ouabain-induced ROS production; this production is involved in regulating the downstream activation of ERK1/2 in LLC-PK1 cells.

Increased expression of NOX2 as an important ROS-generating NOX isoform in ouabain-treated LLC-PK1 cells. The NOX family is a major source of intracellular ROS. To characterize NOX isoforms, the expression levels of NOX1, NOX2, NOX4 and NOX5 were assessed in LLC-PK1 cells. Among the NOX isoforms, the expression of NOX2 was significantly increased with ouabain treatment, while there were no obvious differences in the expression levels of NOX1, NOX4 or NOX5 (Fig. 7A and D-F). In addition, increased expression levels of NOX2 components, such as p67phox and p47phox, were observed, consistent with the changes in NOX2 expression (Fig. 7B and C). As it was demonstrated that NOX2 was upregulated in ouabain-treated LLC-PK1 cells, its role in oxidative stress generation was then examined in a functional study with siRNA-mediated knockdown. Transfection with NOX2 siRNA reduced basal expression of NOX2 by ~50% (Fig. 7G). NADPH-dependent ROS levels were then measured

in cells under basal conditions and after ouabain stimulation. In cells transfected with control siRNA, ouabain significantly increased ROS levels. However, ouabain did not enhance ROS production in cells that had been transfected with NOX2 siRNA (Fig. 7H and I). Thus, NOX2 is likely to have an important role in ROS production in ouabain-treated LLC-PK1 cells.

NOX2/ROS is involved in Src-regulated signaling pathways and trans-differentiation in ouabain-stimulated LLC-PK1 cells. Considering the upregulation of Src and NOX2/ROS in ouabain-stimulated LLC-PK1 cells, their relationship was explored in greater detail. Under basal conditions, PP2 did not influence NOX2 expression. Pretreatment with PP2 (5 μM, 30 min) reduced the ouabain-induced increase in NOX2 expression (Fig. 8A). NOX2 silencing did not affect basal activation of Src or ERK1/2 in LLC-PK1 cells. Transfection with NOX2 siRNA did not significantly reduce ouabain-induced Src activation, although it did inhibit ERK1/2 activation in LLC-PK1 cells (Fig. 8B and C).

As a previous study by our group observed activation of the Na/K-ATPase/Src/ERK1/2 cascade in LLC-PK1 cells to
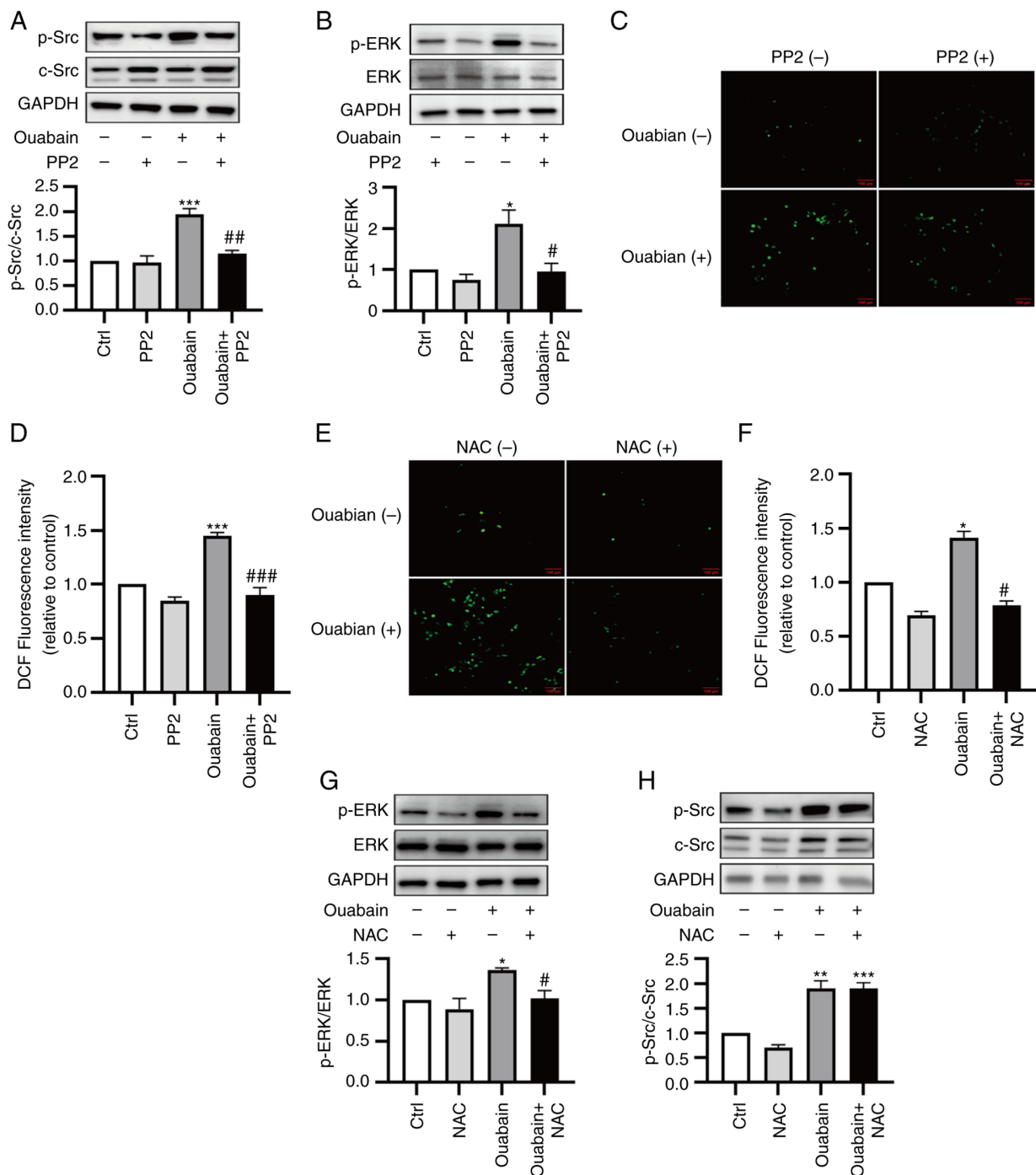
Figure 6. ROS are involved in ouabain-induced activation of Na/K-ATPase/Src/ERK signaling. (A) Effects of PP2 on ouabain-induced Src activation. (B) Effects of PP2 on ouabain-induced ERK activation. (C) Representative fluorescence images of ROS production in PP2-pretreated LLC-PK1 cells (scale bars, 100 μm). (D) DCF fluorescence intensity in PP2-pretreated LLC-PK1 cells. (E) Representative fluorescence images of ROS production in NAC-pretreated LLC-PK1 cells (scale bars, 100 μm). (F) DCF fluorescence intensity in NAC-pretreated LLC-PK1 cells. (G) Effects of NAC on ouabain-induced Src activation. (H) Effects of NAC on ERK activation. Representative western blots and quantitative data are shown. Values are expressed as the mean ± SEM (n=3). $^*P<0.05$; $^{**}P<0.01$; $^{***}P<0.001$ compared with Ctrl; $^#P<0.05$; $^{##}P<0.01$; $^{###}P<0.001$ compared with ouabain. Ctrl, control; NAC, N-acetylcysteine; PP2, 1-tert-butyl-3-(4-chlorophenyl)-1H-pyrazolo[3,4-d]pyrimidin-4-amine; ROS, reactive oxygen species; DCF, dichlorofluorescein.

induce phenotype transformation of LLC-PK1 cells via down-regulation of E-cadherin (17), the role of NOX2 in this process was then investigated. When NOX2 siRNA-transfected cells were treated with ouabain for 24 h, E-cadherin expression was not altered compared with the basal conditions. By contrast, ouabain treatment led to decreased E-cadherin expression in control siRNA-transfected cells. Thus, transfection with

NOX2 siRNA prevented the ouabain-induced downregulation of E-cadherin expression (Fig. 8D).

Discussion

The involvement of the Na/K-ATPase/Src/ROS oxidative amplification loop has been reported in various disease
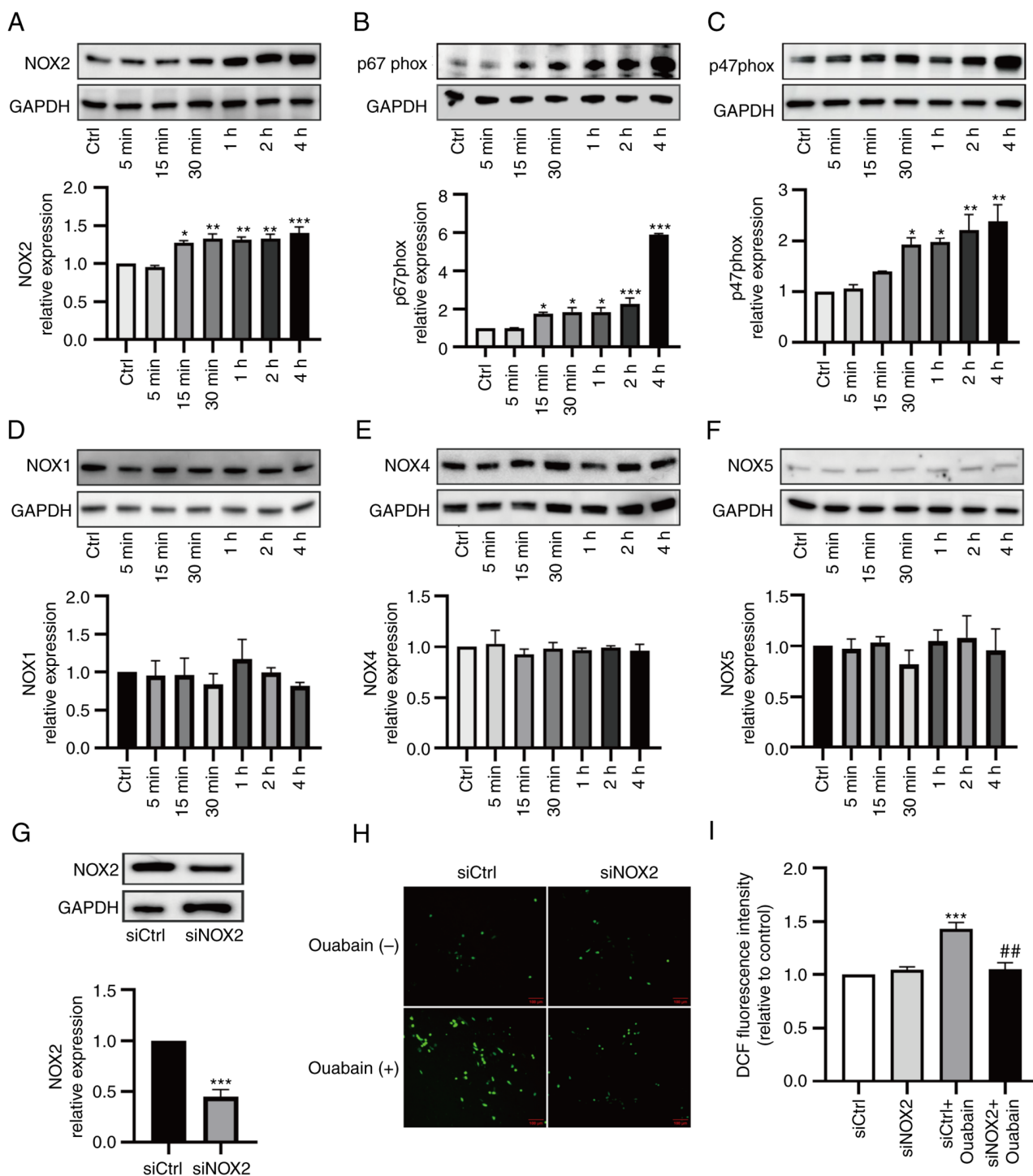
Figure 7. NOX2 is the source of ouabain-induced ROS production. (A) Time course of NOX2 expression. (B) Time course of p67phox expression. (C) Time course of p47phox expression. (D) Time course of NOX1 expression. (E) Time course of NOX4 expression. (F) Time course of NOX5 expression. (G) NOX2 expression was knocked down by siRNA. (H) Representative fluorescence images of ROS production in transfected LLC-PK1 cells with ouabain treatment (scale bars, 100 µm). (I) DCF fluorescence intensity in transfected LLC-PK1 cells with ouabain treatment. Representative western blots and quantitative data are provided. Values are expressed as the mean ± SEM (n=3). *P<0.05; **P<0.01; ***P<0.001 compared with Ctrl or siCtrl; ##P<0.01 compared with ouabain or siCtrl + ouabain. Ctrl, control; siCtrl, control siRNA; siNOX2, NOX2 siRNA; siRNA, small inhibitory RNA; ROS, reactive oxygen species; NOX, NADPH oxidase; DCF, dichlorofluorescein.

models, including uremic cardiomyopathy, cognitive decline and neurodegeneration, salt-sensitive hypertension and obesity (19-23). However, the source of ROS in this loop has remained to be fully elucidated. In the present study, the role of the Na/K-ATPase/Src/ROS oxidative amplification loop and the involvement of NOXs

in renal fibrosis were examined. It was demonstrated that NOXs-derived ROS mediated the Src-regulated signaling cascade for fibrogenic processes, while regulating Na/K-ATPase/Src complex activation, in UUO mice. Experiments with LLC-PK1 cells further clarified the roles of specific NOXs in the Na/K-ATPase/Src/ROS
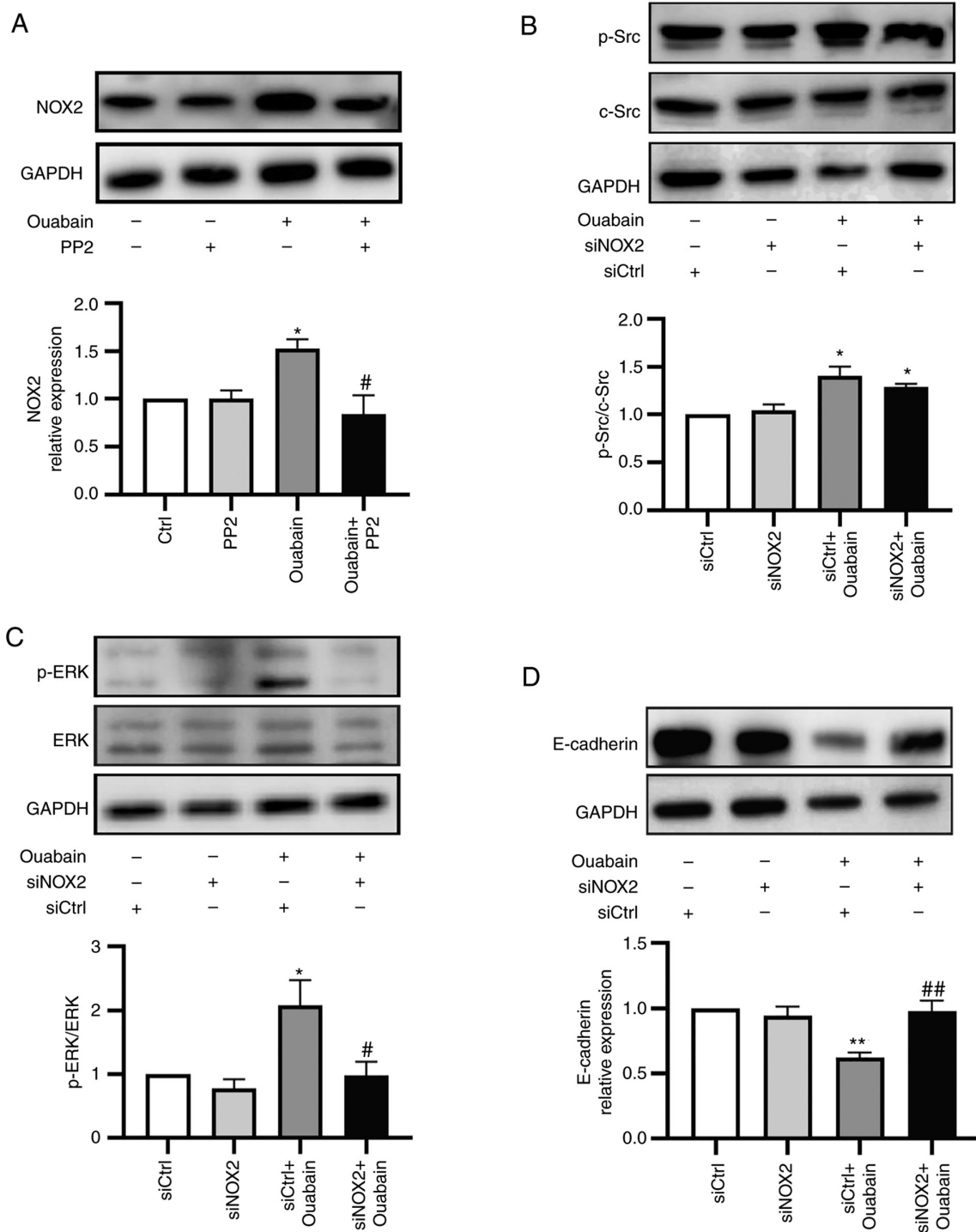
Figure 8. Roles of NOX2/reactive oxygen species in ouabain-induced Na/K-ATPase/Src/ERK signaling and cellular trans-differentiation. (A) Effects of PP2 on NOX2 expression. (B) Effects of NOX2 siRNA on ouabain-induced Src activation. (C) Effects of NOX2 siRNA on ouabain-induced ERK activation. (D) Effects of NOX2 siRNA on E-cadherin expression. Representative western blots and quantitative data are shown. Values are expressed as the mean ± SEM (n=3). *P<0.05; **P<0.01 compared with Ctrl; #P<0.05; ##P<0.01 compared with ouabain or siCtrl + ouabain. Ctrl, control; siCtrl, control siRNA; siNOX2, NOX2 siRNA; siRNA, small inhibitory RNA; PP2, 1-tert-butyl-3-(4-chlorophenyl)-1H-pyrazolo[3,4-d]pyrimidin-4-amine; NOX, NADPH oxidase.

oxidative amplification loop via NOX2 silencing with siRNA. It was found that NOX2-induced ROS production was Na/K-ATPase/Src-dependent in ouabain-stimulated cells; it was associated with downstream activation of the Src signaling pathway and cellular transdifferentiation. Collectively, the present results revealed that NOXs are key mediators of the Na/K-ATPase/Src/ROS oxidant amplification loop involved in renal fibrosis.

Renal fibrosis is the final common pathological manifestation of chronic kidney disease resulting from various etiologies. UUO is the most widely used model of interstitial fibrosis. While the UUO model has certain limitations, such as the rarity of absolute obstruction in humans, its lack of applicability to certain renal fibrosis conditions and its inability to monitor changes in renal function, the model also has several advantages. These advantages include high reproducibility,

ease of implementation, a rapid time course and the capacity to replicate a fibrotic sequence of events closely resembling the pathogenesis in humans (31). Accordingly, the UUO model was utilized as an example of renal interstitial fibrosis in the present study.

Src kinase is a versatile non-receptor protein tyrosine kinase that regulates numerous intracellular signaling cascades upon activation by growth factors/cytokines from diverse membrane receptors (5-7). There is evidence that Src activation is involved in numerous renal lesions in animal models, including the model of renal fibrosis (7,9,10). In the present study, inhibition of Src activation by PP2 alleviated myofibroblast accumulation and extracellular matrix deposition in UUO-induced renal fibrosis, supporting the central role of Src in fibrosis onset.

In addition to its well-known pump function, Na/K-ATPase has been identified as a regulator of Src kinase in recent years. The $\alpha1$ subunit of Na/K-ATPase binds to Src to form the Na/K-ATPase/Src complex; this interaction maintains Src in an inactive state (32,33). When the Na/K-ATPase conformation is altered via ligand binding or the expression of Na/K-ATPase decreases, Src is released and activated (34-36). Increased ROS production has been observed upon activation of the Na/K-ATPase/Src complex. Meanwhile, there is emerging evidence that the Na/K-ATPase/Src complex may be activated by ROS in addition to classic ligands for Na/K-ATPase (e.g., cardiotonic steroids) (14-17,37). Therefore, an oxidant amplification loop may exist between oxidative stress and the Na/K-ATPase/Src complex. When the Na/K-ATPase/Src complex is activated, a signaling cascade is initiated; this results in ROS generation and subsequent activation of the Na/K-ATPase/Src complex, thereby forming a reciprocal regulatory process (12,14). Studies have indicated that this Na/K-ATPase oxidant amplification loop is involved in diseases such as uremic cardiomyopathy, obesity, aging, cognitive decline and neurodegeneration, and cardiovascular disease (19-23). A previous study by our group found that the UUO-induced increase in 8-iso-prostaglandin F2α expression was reduced by pNaKtide treatment, suggesting that oxidative stress in Na/K-ATPase-mediated signaling is involved in UUO-induced renal fibrosis (10). ROS are difficult to directly measure because of their short half-lives. ROS-induced oxidative stress may cause oxidative damage in organelles (e.g. mitochondria) and biomolecules such as proteins, lipids and DNA (38,39). In general, macromolecules produced by ROS activity are used as markers for estimation of oxidative stress (40). In the present study, levels of 3-NT, 4-HNE, 8-OHdG, Nrf2 and HO-1 were measured to determine ROS production. It was found that oxidative stress was reduced in PP2-treated UUO mice; Src-regulated signaling pathway inhibition in apocynin-treated UUO mice was also observed. Furthermore, apocynin administration partially reversed the downregulation of Na/K-ATPase expression in UUO mice. Collectively, these *in vivo* findings suggested that an Na/K-ATPase/Src/ROS oxidant amplification loop is involved in UUO-induced renal fibrosis.

The source of ROS involved in the oxidant amplification loop has not been elucidated thus far. The NOX family consists of seven isoforms; NOX1, NOX2, NOX4 and NOX5 have the highest expression in renal cells (26,41-43). The
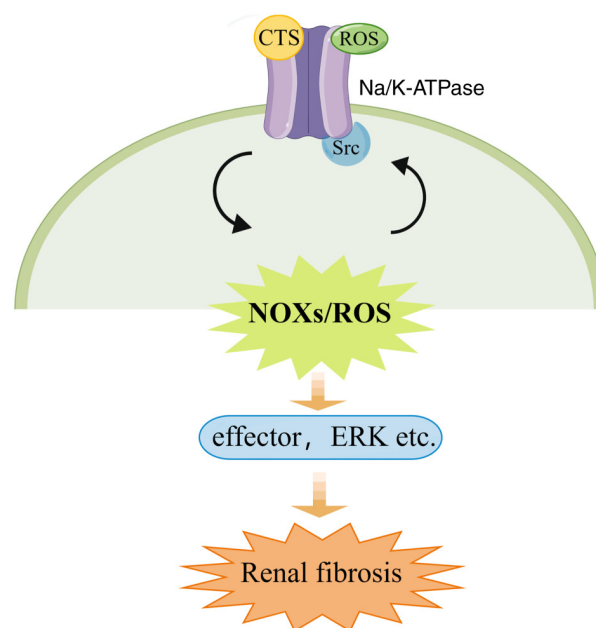

Figure 9. Schematic illustration of the mechanism of the Na/K-ATPase/Src/ROS oxidant amplification loop in renal fibrosis (created with FigDraw). CTS, cardiotonic steroids; NOXs, NADPH oxidases; ROS, reactive oxygen species.

levels of NOXs are elevated in several models of acute kidney injury and chronic kidney disease, leading to excess ROS production (37,44-46). In a previous study by our group, it was observed that both NOX2 and NOX4 were upregulated and NOX activity was increased in UUO model mice (28). Apocynin exerts an antioxidant effect by inhibiting NOXs. The attenuation of NOXs led to lower oxidative stress and a decrease in UUO-induced renal fibrosis, suggesting that NOXs constitute an important source of ROS in the UUO model (29). In the present study, it was experimentally confirmed that NOX-derived ROS generation was increased in UUO model mice; an interaction between NOX regulation and the Src-regulated signaling cascade in renal fibrosis was demonstrated. As expected, apocynin administration significantly reduced the upregulation of NOX2 and NOX4, which led to decreased levels of oxidative stress biomarkers in UUO mice. Furthermore, apocynin treatment partially reversed the downregulation of Na/K-ATPase expression and significantly inhibited the activation of Src and downstream ERK. Furthermore, PP2-induced inhibition of Src attenuated the upregulation of NOX2, NOX4 and oxidative stress biomarkers to a level comparable with the results of apocynin treatment in UUO mice. These findings suggest that interactions between NOXs/ROS and Src activation are involved in renal fibrosis.

Because the activation of Src and NOXs may be simultaneously affected by convergent stimuli *in vivo*, the specific roles of NOXs in the Na/K-ATPase/Src oxidant amplification loop in LLC-PK1 cells were subsequently examined. Crosstalk between Na/K-ATPase/Src and NOXs has been demonstrated in various cell types. Liu *et al* (47) found that angiotensin II inhibited the Na/K-ATPase pump in vascular smooth muscle cells via NADPH oxidase-dependent glutathionylation of the β1 subunit of Na/K-ATPase. Weaver *et al* (48) reported that

NOX1 expression was regulated by a ROS- and Src-mediated feed-forward loop in beta cells. Camargo *et al* (49) demonstrated that NOX5 mediated the Src oxidant amplification loop in human vascular cells. Li *et al* (50) observed a reciprocal relationship between NOX1/NOX2 and c-Src activation in fibroblasts after hypoxia/reoxygenation. Furthermore, Yan *et al* (51) reported that NOXs were the source of ouabain-induced ROS in myocardial cells. In the present study, a cellular model using ouabain, a classical ligand for Na/K-ATPase, was generated to stimulate LLC-PK1 cells. LLC-PK1 cells were chosen due to their higher sensitivity to ouabain compared to human or rodent cells, as well as the availability of accumulated data from studies concerning the Na-K-ATPase/Src (13,52). The present results revealed that ouabain-induced Src/ERK activation and the simultaneous increases in NOX2 expression and ROS generation in LLC-PK1 cells were suppressed by PP2 pretreatment, supporting the notion that ROS production in LLC-PK1 cells involves an Src-dependent process. The interaction between P47phox and p67phox with NOX2 is critical for the formation of an active NOX2 functional complex (41). In addition to the detection of increased NOX2 expression, a paralleled increase in the expression levels of p47phox and p67phox was also observed after ouabain stimulation, supporting the role of NOX2 as the source of ouabain-induced ROS production. NOX2 siRNA prevented ouabain-induced ROS production and ERK activation without influencing ouabain-induced Na/K-ATPase/Src activation, suggesting that NOX2 has a role in mediating the Src downstream signaling pathway via ROS production. To explore the functional implications of the Na/K-ATPase/Src/NOXs/ROS axis, the phenotypic differentiation of LLC-PK1 cells was examined. NOX2 silencing partially reversed the ouabain-induced downregulation of E-cadherin expression. In contrast to the *in vivo* findings, no significant changes in NOX4 expression were detected in ouabain-stimulated LLC-PK1 cells. This discrepancy may be related to species differences or to the involvement of various NOX isoforms in the Na/K-ATPase/Src/ROS amplification loop across a diverse range of cell types that contribute to renal fibrosis. For instance, NOX4 is continuously activated in vascular smooth muscle cells for production of intracellular ROS under basal conditions (53). Furthermore, no changes in NOX1 or NOX5 expression were detected. Taken together, these findings suggested that NOX2 was the major source of ouabain-induced ROS in LLC-PK1 cells.

Mitochondria represent another major source of ROS in the kidney. Liu *et al* (18) indicated that mitochondria were involved in ouabain-induced ROS production in myocardial cells. In the present study, the effect of mitochondria on ROS production was not evaluated. Of note, interactions between mitochondria and NOXs have been described. In models of acute kidney injury and chronic kidney disease, the use of apocynin, a NOX inhibitor, decreased mitochondrial ROS production (54,55); this finding supports the notion that crosstalk between NOXs and mitochondria is involved in establishing a pathological cycle of ROS production.

In conclusion, in the present study, NOXs were identified as a major source of oxidative stress and a mediator of the Na/K-ATPase/Src/ROS oxidant amplification loop in renal fibrosis. ROS are produced via NOX activation after activation of the Na/K-ATPase/Src complex, which in return activates the Na/K-ATPase/Src complex and mediates Src-regulated downstream signaling cascades and fibrogenic effects (Fig. 9). The disruption of this vicious feed-forward loop between NOXs/ROS and redox-regulated Na/K-ATPase/Src may have therapeutic applicability for renal fibrosis disorders.

Availability of data and materials

The datasets used and/or analyzed during the current study are available from the corresponding author on reasonable request.

Authors' contributions

HZ, FL and XC performed the experiments and analyzed the data. YW designed the experiments, interpreted the data and wrote the manuscript. HZ and YW confirmed the authenticity of all the raw data. All authors have read and approved the final manuscript.

Ethics approval and consent to participate

All animal experiments were approved by the Animal Experimentation Ethics Committee of Peking University First Hospital (Beijing, China; approval no. J2022005).

Patient consent for publication

Not applicable.

Competing interests

The authors declare that they have no competing interests.

References

1. Wang T, Cui S, Liu X, Han L, Duan X, Feng S, Zhang S and Li G: LncTUG1 ameliorates renal tubular fibrosis in experimental diabetic nephropathy through the miR-145-5p/dual-specificity phosphatase 6 axis. Ren Fail 45: 2173950, 2023.
2. Wang W, Sheng L, Chen Y, Li Z, Wu H, Ma J, Zhang D, Chen X and Zhang S: Total coumarin derivates from Hydrangea paniculata attenuate renal injuries in cationized-BSA induced membranous nephropathy by inhibiting complement activation and interleukin 10-mediated interstitial fibrosis. Phytomedicine 96: 153886, 2022.
3. Webster AC, Nagler EV, Morton RL and Masson P: Chronic kidney disease. Lancet 389: 1238-1252, 2017.
4. Zhang S, Yang J, Li H, Li Y, Liu Y, Zhang D, Zhang F, Zhou W and Chen X: Skimmin, a coumarin, suppresses the streptozotocin-induced diabetic nephropathy in wistar rats. Eur J Pharmacol 692: 78-83, 2012.
5. Zhou D and Liu Y: Therapy for kidney fibrosis: Is the Src kinase a potential target? Kidney Int 89: 12-14, 2016.
6. Li N, Lin G, Zhang H, Sun J, Gui M, Liu Y, Li W, Liu J and Tang J: Src family kinases: A potential therapeutic target for acute kidney injury. Biomolecules 12: 984, 2022.

7. Wang J and Zhuang S: Src family kinases in chronic kidney disease. Am J Physiol Renal Physiol 313: F721-F728, 2017.
8. Roskoski R Jr: Src protein-tyrosine kinase structure, mechanism, and small molecule inhibitors. Pharmacol Res 94: 9-25, 2015.
9. Yan Y, Ma L, Zhou X, Ponnusamy M, Tang J, Zhuang MA, Tolbert E, Bayliss G, Bai J and Zhuang S: Src inhibition blocks renal interstitial fibroblast activation and ameliorates renal fibrosis. Kidney Int 89: 68-81, 2016.
10. Cheng X, Song Y and Wang Y: pNaKtide ameliorates renal interstitial fibrosis through inhibition of sodium-potassium adenosine triphosphatase-mediated signaling pathways in unilateral ureteral obstruction mice. Nephrol Dial Transplant 34: 242-252, 2019.
11. Li Z and Xie Z: The Na/K-ATPase/Src complex and cardiotonic steroid-activated protein kinase cascades. Pflugers Arch 457: 635-644, 2009.
12. Pratt RD, Brickman CR, Cottrill CL, Shapiro JI and Liu J: The Na/K-ATPase signaling: From specific ligands to general reactive oxygen species. Int J Mol Sci 19: 2600, 2018.
13. Lai F, Madan N, Ye Q, Duan Q, Li Z, Wang S, Si S and Xie Z: Identification of a mutant α1 Na/K-ATPase that pumps but is defective in signal transduction. J Biol Chem 288: 13295-13304, 2013.
14. Yan Y, Shapiro AP, Haller S, Katragadda V, Liu L, Tian J, Basrur V, Malhotra D, Xie ZJ, Abraham NG, *et al*: Involvement of reactive oxygen species in a feed-forward mechanism of Na/K-ATPase-mediated signaling transduction. J Biol Chem 288: 34249-34258, 2013.
15. Xie Z, Kometiani P, Liu J, Li J, Shapiro JI and Askari A: Intracellular reactive oxygen species mediate the linkage of Na+/K+-ATPase to hypertrophy and its marker genes in cardiac myocytes. J Biol Chem 274: 19323-19328, 1999.
16. Liu L, Li J, Liu J, Yuan Z, Pierre SV, Qu W, Zhao X and Xie Z: Involvement of Na+/K+-ATPase in hydrogen peroxide-induced hypertrophy in cardiac myocytes. Free Radic Biol Med 41: 1548-1556, 2006.
17. Wang Y, Ye Q, Liu C, Xie JX, Yan Y, Lai F, Duan Q, Li X, Tian J and Xie Z: Involvement of Na/K-ATPase in hydrogen peroxide-induced activation of the Src/ERK pathway in LLC-PK1 cells. Free Radic Biol Med 71: 415-426, 2014.
18. Liu J, Tian J, Haas M, Shapiro JI, Askari A and Xie Z: Ouabain interaction with cardiac Na+/K+-ATPase initiates signal cascades independent of changes in intracellular Na+ and Ca2+ concentrations. J Biol Chem 275: 27838-27844, 2000.
19. Bartlett DE, Miller RB, Thiesfeldt S, Lakhani HV, Shapiro JI and Sodhi K: The role of Na/K-atpase signaling in oxidative stress related to aging: Implications in obesity and cardiovascular disease. Int J Mol Sci 19: 2139, 2018.
20. Shah PT, Martin R, Yan Y, Shapiro JI and Liu J: Carbonylation modification regulates Na/K-ATPase signaling and salt sensitivity: A review and a hypothesis. Front Physiol 7: 256, 2016.
21. Sodhi K, Pratt R, Wang X, Lakhani HV, Pillai SS, Zehra M, Wang J, Grover L, Henderson B, Denvir J, *et al*: Role of adipocyte Na,K-ATPase oxidant amplification loop in cognitive decline and neurodegeneration. iScience 24: 103262, 2021.
22. Liu J, Yan Y, Liu L, Xie Z, Malhotra D, Joe B and Shapiro JI: Impairment of Na/K-ATPase signaling in renal proximal tubule contributes to Dahl salt-sensitive hypertension. J Biol Chem 286: 22806-22813, 2011.
23. Sodhi K, Wang X, Chaudhry MA, Lakhani HV, Zehra M, Pratt R, Nawab A, Cottrill CL, Snoad B, Bai F, *et al*: Central role for adipocyte Na,K-ATPase oxidant amplification loop in the pathogenesis of experimental uremic cardiomyopathy. J Am Soc Nephrol 31: 1746-1760, 2020.
24. Jha JC, Dai A, Garzarella J, Charlton A, Urner S, Østergaard JA, Okabe J, Holterman CE, Skene A, Power DA, *et al*: Independent of Renox, NOX5 promotes renal inflammation and fibrosis in diabetes by activating ROS-sensitive pathways. Diabetes 71: 1282-1298, 2022.
25. Alhasson F, Seth RK, Sarkar S, Kimono DA, Albadrani MS, Dattaroy D, Chandrashekaran V, Scott GI, Raychoudhury S, Nagarkatti M, *et al*: High circulatory leptin mediated NOX-2-peroxynitrite-miR21 axis activate mesangial cells and promotes renal inflammatory pathology in nonalcoholic fatty liver disease. Redox Biol 17: 1-15, 2018.
26. Holterman CE, Read NC and Kennedy CRJ: Nox and renal disease. Clin Sci (Lond) 128: 465-481, 2015.
27. Eid AA, Gorin Y, Fagg BM, Maalouf R, Barnes JL, Block K and Abboud HE: Mechanisms of podocyte injury in diabetes: Role of cytochrome P450 and NADPH oxidases. Diabetes 58: 1201-1211, 2009.
28. Liu C, Song Y, Qu L, Tang J, Meng L and Wang Y: Involvement of NOX in the regulation of renal tubular expression of Na/K-ATPase in acute unilateral ureteral obstruction rats. Nephron 130: 66-76, 2015.
29. Cheng X, Zheng X, Song Y, Qu L, Tang J, Meng L and Wang Y: Apocynin attenuates renal fibrosis via inhibition of NOXs-ROS-ERK-myofibroblast accumulation in UUO rats. Free Radic Res 50: 840-852, 2016.
30. Liu M, Liu T, Shang P, Zhang Y, Liu L, Liu T and Sun S: Acetyl-11-keto-β-boswellic acid ameliorates renal interstitial fibrosis via Klotho/TGF-β/Smad signalling pathway. J Cell Mol Med 22: 4997-5007, 2018.
31. Nogueira A, Pires MJ and Oliveira PA: Pathophysiological mechanisms of renal fibrosis: A review of animal models and therapeutic strategies. In Vivo 31: 1-22, 2017.
32. Tian J, Cai T, Yuan Z, Wang H, Liu L, Haas M, Maksimova E, Huang XY and Xie ZJ: Binding of Src to Na+/K+-ATPase forms a functional signaling complex. Mol Biol Cell 17: 317-326, 2006.
33. Cui X and Xie Z: Protein interaction and Na/K-ATPase-mediated signal transduction. Molecules 22: 990, 2017.
34. Shinoda T, Ogawa H, Cornelius F and Toyoshima C: Crystal structure of the sodium-potassium pump at 2.4 A resolution. Nature 459: 446-450, 2009.
35. Laursen M, Yatime L, Nissen P and Fedosova NU: Crystal structure of the high-affinity Na+K+-ATPase-ouabain complex with Mg2+ bound in the cation binding site. Proc Natl Acad Sci USA 110: 10958-10963, 2013.
36. Xie JX, Li X and Xie Z: Regulation of renal function and structure by the signaling Na/K-ATPase. IUBMB Life 65: 991-998, 2013.
37. Yan Y, Shapiro AP, Mopidevi BR, Chaudhry MA, Maxwell K, Haller ST, Drummond CA, Kennedy DJ, Tian J, Malhotra D, *et al*: Protein carbonylation of an amino acid residue of the Na/K-ATPase α1 subunit determines Na/K-ATPase signaling and sodium transport in renal proximal tubular cells. J Am Heart Assoc 5: e003675, 2016.
38. Lv W, Booz GW, Fan F, Wang Y and Roman RJ: Oxidative stress and renal fibrosis: Recent insights for the development of novel therapeutic strategies. Front Physiol 9: 105, 2018.
39. Zhang Y, Li Z, Wu H, Wang J and Zhang S: Esculetin alleviates murine lupus nephritis by inhibiting complement activation and enhancing Nrf2 signaling pathway. J Ethnopharmacol 288: 115004, 2022.
40. Demirci-Çekiç S, Özkan G, Avan AN, Uzunboy S, Çapanoğlu E and Apak R: Biomarkers of oxidative stress and antioxidant defense. J Pharm Biomed Anal 209: 114477, 2022.
41. Bedard K and Krause KH: The NOX family of ROS-generating NADPH oxidases: Physiology and pathophysiology. Physiol Rev 87: 245-313, 2007.
42. Gill PS and Wilcox CS: NADPH oxidases in the kidney. Antioxid Redox Signal 8: 1597-1607, 2006.
43. Aranda-Rivera AK, Cruz-Gregorio A, Aparicio-Trejo OE, Ortega-Lozano AJ and Pedraza-Chaverri J: Redox signaling pathways in unilateral ureteral obstruction (UUO)-induced renal fibrosis. Free Radic Biol Med 172: 65-81, 2021.
44. Lee SR, An EJ, Kim J and Bae YS: Function of NADPH oxidases in diabetic nephropathy and development of Nox inhibitors. Biomol Ther (Seoul) 28: 25-33, 2020.
45. Shin HS, Yu M, Kim M, Choi HS and Kang DH: Renoprotective effect of red ginseng in gentamicin-induced acute kidney injury. Lab Invest 94: 1147-1160, 2014.
46. Yoo JY, Cha DR, Kim B, An EJ, Lee SR, Cha JJ, Kang YS, Ghee JY, Han JY and Bae YS: LPS-induced acute kidney injury is mediated by Nox4-SH3YL1. Cell Rep 33: 108245, 2020.
47. Liu CC, Karimi Galougahi K, Weisbrod RM, Hansen T, Ravaie R, Nunez A, Liu YB, Fry N, Garcia A, Hamilton EJ, *et al*: Oxidative inhibition of the vascular Na+-K+ pump via NADPH oxidase-dependent β1-subunit glutathionylation: implications for angiotensin II-induced vascular dysfunction. Free Radic Biol Med 65: 563-572, 2013.
48. Weaver JR and Taylor-Fishwick DA: Regulation of NOX-1 expression in beta cells: A positive feedback loop involving the Src-kinase signaling pathway. Mol Cell Endocrinol 369: 35-41, 2013.
49. Camargo LL, Montezano AC, Hussain M, Wang Y, Zou Z, Rios FJ, Neves KB, Alves-Lopes R, Awan FR, Guzik TJ, *et al*: Central role of c-Src in NOX5-mediated redox signalling in vascular smooth muscle cells in human hypertension. Cardiovasc Res 118: 1359-1373, 2022.
50. Li Q, Zhang Y, Marden JJ, Banfi B and Engelhardt JF: Endosomal NADPH oxidase regulates c-Src activation following hypoxia/reoxygenation injury. Biochem J 411: 531-541, 2008.

51. Yan X, Xun M, Dou X, Wu L, Han Y and Zheng J: Regulation of Na$^+$-K$^+$-ATPase effected high glucose-induced myocardial cell injury through c-Src dependent NADPH oxidase/ROS pathway. Exp Cell Res 357: 243-251, 2017.
52. Yan Y, Haller S, Shapiro A, Malhotra N, Tian J, Xie Z, Malhotra D, Shapiro JI and Liu J: Ouabain-stimulated trafficking regulation of the Na/K-ATPase and NHE3 in renal proximal tubule cells. Mol Cell Biochem 367: 175-183. 2012.
53. Clempus RE, Sorescu D, Dikalova AE, Pounkova L, Jo P, Sorescu GP, Schmidt HH, Lassègue B and Griendling KK: Nox4 is required for maintenance of the differentiated vascular smooth muscle cell phenotype. Arterioscler Thromb Vasc Biol 27: 42-48, 2007.
54. Kozieł R, Pircher H, Kratochwil M, Lener B, Hermann M, Dencher NA and Jansen-Dürr P: Mitochondrial respiratory chain complex I is inactivated by NADPH oxidase Nox4. Biochem J 452: 231-239, 2013.
55. Fukai T and Ushio-Fukai M: Cross-talk between NADPH oxidase and mitochondria: Role in ROS signaling and angiogenesis. Cells 9: 1849. 2020.